Polyhedron 52 (2013) 1385–1390

Contents lists available at SciVerse ScienceDirect

Polyhedron

journal homepage: www.elsevier.com/locate/poly

Adenine supported hydroxyl-bridged dicopper core as a catalytically competent unit for phenol oxidation

Ashutosh Kumar Mishra, Rajneesh Kumar Prajapati, Sandeep Verma *

Department of Chemistry, Indian Institute of Technology Kanpur, Kanpur 208016, UP, India

ARTICLE INFO

Article history:
Available online 30 May 2012

Dedicated to 100th Anniversary of the 1913 Nobel Prize in Chemistry to Alfred Werner

Keywords:
Propyladenine
Dicopper core
Phenol oxidation

ABSTRACT

This communication describes crystallographic investigation of a dicopper complex of modified adenine nucleobase containing a Cu_2O_2 core. This arrangement is remarkably similar to active sites present in some copper-containing redox enzymes. Interestingly, this complex is also competent in catalyzing redox reactions, suggesting the possibility of catalytically competent primitive metal-nucleobase systems.

1. Introduction

Studies involving metal–adenine interactions have attracted considerable attention owing to the presence of heterocyclic ring, which can support coordination leading to the formation of varied motifs with potential applications in generating metal–nucleobase frameworks and aiding catalysis of certain reactions [1]. The heterocyclic ring of adenine can be dissected into two unequal halves of six- and five-membered rings. The former supports Watson–Crick hydrogen bonding, while the five membered ring invoked for the Hoogsteen base-pairing resembles imidazole side-chain of histidine amino acid offering a nucleophilic site and general acid–base framework [2]. Thus, adenine has been implicated in synthetic metalated motifs exhibiting catalytic actions such as catalase-like activity for hydrogen peroxide disproportionation [3], and phosphate ester hydrolysis reaction [4], to name a few. Systematic studies conducted by us to explore silver coordination chemistry of substituted adenine nucleobase have resulted in the formation of several novel frameworks [5,6]. In this process, we have discovered that N9-alkyl substituents display a marked preference for silver metallaquartets [5a,b,j]; a carboxyl substituent supports silver containing hexamer formation [5e]; a cyanoethyl substituent yields an interconnected metal-nucleobase framework [5i]; while a thiocyanatoethyl substituent leads to CuI aggregates [5l]. In addition, our earlier studies had also revealed interesting catalytic activities [4b–e,6]. The present report describes synthesis and crystallographic investigation of copper complex of 9-propyladenine (**1**), containing a hydroxyl-bridged dicopper core and its ability to catalyze phenol oxidation reactions.

2. Material and methods

N,*N*-dimethylformamide was distilled prior to use. ^1H and ^{13}C NMR were recorded on JEOL-JNM LAMBDA 400 model operating at 400, 100 MHz, respectively. HRMS mass spectra for the ligand and metalated complexes were recorded at IIT Kanpur, India, on Waters, Q-Tof Premier Micromass HAB 213 mass spectrometer using capillary voltage 2.6–3.2 kV. Solvents were evaporated using rotary evaporator under reduce pressure. NaH was purchased from sd fine chemicals Pvt. Ltd. Mumbai, India, *n*-propyl bromide was purchased from Spectrochem Pvt. Ltd. Mumbai; 6-chloropurine was purchased from SRL, India and used without further purification. All solvents were distilled prior to use using standards procedures.

2.1. Synthesis of 9-propyladenine (9-PA)

Synthesis of 9-PA was carried out by a previously reported procedure [5b]. In brief, adenine (2.0 g, 14.8 mmol) was dissolved in DMF (10 mL), followed by addition of NaH (0.71 g as 60% in paraffin, 17.7 mmol) and stir under nitrogen atmosphere for 30 min. After this *n*-propyl bromide (1.33 mL, 14.0 mmol) is added and stir overnight under nitrogen atmosphere. After this time, DMF is evaporated under high vacuum and compound is separated by column chromatography (1.05 g, 40% yield). FABMS: $(M^+ + 1) = 178$; M.P. = 167 °C. ^1H NMR: (400 MHz, $CDCl_3$, 22 °C, TMS) δ (ppm) 0.88–0.92 (t, 3H), 1.84–1.91 (m, 2H), 4.09–4.12 (t, 2H), 6.14 (s,

* Corresponding author.
E-mail address: sverma@iitk.ac.in (S. Verma).

0277-5387/$ - see front matter © 2012 Elsevier Ltd. All rights reserved.
http://dx.doi.org/10.1016/j.poly.2012.05.013

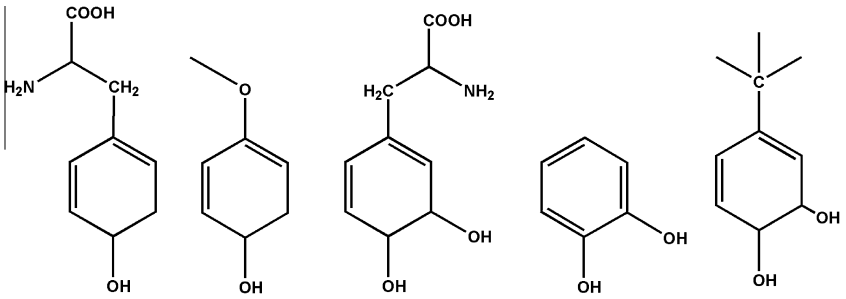

Scheme 1. Schematic representation of different substrates used.

Table 1
Crystallographic data for 9-propyladenine (9-PA) and its copper complex (**1**).

Identification code	9-PA	9-PA copper complex
Empirical formula	$C_8H_{11}N_5$	$C_{64}H_{104}Cl_{12}Cu_4N_{40}O_{56}$
Mr	177.22	3009.43
Crystal system	monoclinic	monoclinic
Space group	*P* 21/*c*	*P* 21/*n*
a (Å)	8.4744 (9)	18.274 (3)
b (Å)	14.2188 (14)	14.433 (3)
c (Å)	14.3922 (14)	21.692 (4)
α (°)	90	90
β (°)	92.091 (2)	100.46 (3)
λ (°)	90	90
V (A^3)	1733.0 (3)	5626.2 (18)
D_{calc} (mg m^{-3})	1.358	1.776
Z	8	8
μ (Mo Kα) (mm^{-1})	0.091	1.147
F (000)	752	3072
2θ range	2.01–28.30	2.14–26.0
Reflection measured	11326	31070
Independent reflection	4266; [R_{int} = 0.0631]	11010; [R_{int} = 0.0593]
Reflection observed ($I > 2\sigma(I)$)	2519	7559
Parameters	235	813
Final R_1, wR_2 (observed data)	R_1 = 0.0651; wR_2 = 0.1218	R_1 = 0.0523; *wR*2 = 0.1232
Goodness-of-fit (observed data)	1.069	1.002
CCDC number*	659665	789919

2H, D_2O exchange), 7.75 (s, 1H), 8.30 (s, 1H). ^{13}C NMR (100 MHz, DMSO-d_6, 20.9 °C, TMS); δ (ppm) 10.94, 22.78, 44.51, 118.76, 140.93, 149.58, 152.38, 155.97. Anal. Calc for $C_8H_{11}N_5$; C, 54.22; H, 6.26; N, 39.52; found C, 54.17; H, 6.22; N, 39.58.

2.2. Procedure for metalation of **1**

9-PA (0.1 g, 0.145 mmol) was dissolved in methanol (3 mL), followed by addition of methanolic solution of copper chloride (0.04 g, 0.3 mmol) and stir for 30 min. After this, solvent is evaporated and the greenish solid thus obtained is washed with water (4 × 5 mL) and methanol (4 × 5 mL) to remove any traces of unreacted metal salt and ligand. After this, 20 μL of perchloric acid was added and left for 1 h. The solvent is evaporated and product so obtained is dried under high vacuum. HRMS: $[4L+2Cu+2O+CH_3OH]^+$ calculated: 882.2861, found 882.5978.

2.3. EPR studies for **1**

EPR spectra were recorded with a Varian E-109 C spectrometer fitted with a quartz dewar for measurements at 120 K. The spectra were calibrated with the help of DPPH (*g* = 2.0037).

Table 2
Selected hydrogen bond distances (Å) and bond angles (°) in **1**.

Complex **1**			
D–H···A[a]	$d_{H\cdots A}$	$d_{D\cdots A}$	angle
N1–H1···OW2	1.92	2.73(4)	158
O1–H1′···O14^{i}	2.08 (4)	2.89(4)	171(4)
N6B–H6B1···O18^{ii}	2.14	2.88(4)	146
N1A–H1A···O18^{ii}	2.15	2.89(4)	145
N1C–H1C···OW1^{ii}	1.96	2.74(4)	152
N1D–H1D···O22	2.15	2.89(4)	145
O2–H2′···O24^{iii}	2.04(4)	2.85(4)	166(6)
N6B–H6B2···O2	2.10	2.85(4)	146
N6C–H6C1···O15^{ii}	2.11	2.95(4)	166
N6C–H6C2···O3	2.18	2.98(4)	155
N6D–H6D1···O22	2.17	2.91(4)	143
N6D–H6D2···O1	2.24	2.96(4)	143
N6–H6A···O20	2.08	2.92(4)	168
N6–H6B···O7	2.27	3.09(4)	161
OW1–H1W1···O17	2.27	3.01(4)	146(3)
OW2–H1W2···O21	2.38 (4)	3.02(4)	131(4)
OW2–H1W2···O11^{i}	2.47(4)	3.10(4)	131(4)
OW1–H2W1···O19^{i}	2.07(3)	3.90(4)	161(4)
OW2–H2W2···O16^{i}	2.15(3)	2.94(4)	157(3)
C2A–H2A···O9^{iv}	2.44	3.35(5)	169
C2D–H2D···O5^{v}	2.52	3.43(5)	168
C8–H8···O25^{i}	2.33	3.15(5)	148
C8A–H8A···OW2^{vi}	2.44	3.27(5)	150
C8C–H8C···O13	2.54	3.26(5)	135
C8D–H8D···OW1	2.56	3.37(5)	146
C8C–H8C···O13	2.54	3.26(5)	135
C14–H14A···N3C^{iv}	2.48	3.29(5)	141
C14–H14B···O21^{vi}	2.54	3.42(5)	153
C21–H21B···N3^{v}	2.42	3.37(5)	170
C23–H23A···O8^{i}	2.33	3.28(5)	172

[a] Symmetry of A: (i) 1/2−*x*,1/2+*y*,1/2−*z*; (ii) −*x*,1−*y*,1−*z*; (iii) −1+*x*,*y*,*z*; (iv) −1/2−*x*,1/2+*y*,1/2−*z*; (v) 1/2−*x*,−1/2+*y*,1/2−*z*; (vi) −*x*,1−*y*, −*z*.

2.4. Phenol oxidation assay

A spectrophotometric assay for **1** with three substrates, catechol, 4-hydroxyanisole, and 4-*t*-butylcatechol, along with a natural monophenolic and diphenolic substrate, tyrosine and L-DOPA respectively (Scheme 1), was used to evaluate the catalytic behaviour of **1** towards phenol oxidation. 0.1 mM solution of **1** prepared in methanol was used for assay. Detailed procedure for each substrate is shown as under:

2.3.1. Catechol oxidation

Solutions of catechol (0.04–0.1 mM) were prepared in 50% aq. methanol. 1% MBTH solution was prepared in methanol. The formation of MBTH–quinone adduct was monitored at 500 nm ($\varepsilon = 3.25 \times 10^4\ M^{-1}\ cm^{-1}$) [7].

2.3.2. 4-Hydroxyanisole (4HA) oxidation

Solutions of 4-HA (2–8 mM) were prepared in 50% aq. methanol containing 2% DMF to ensure the solubility of MBTH-adduct. The

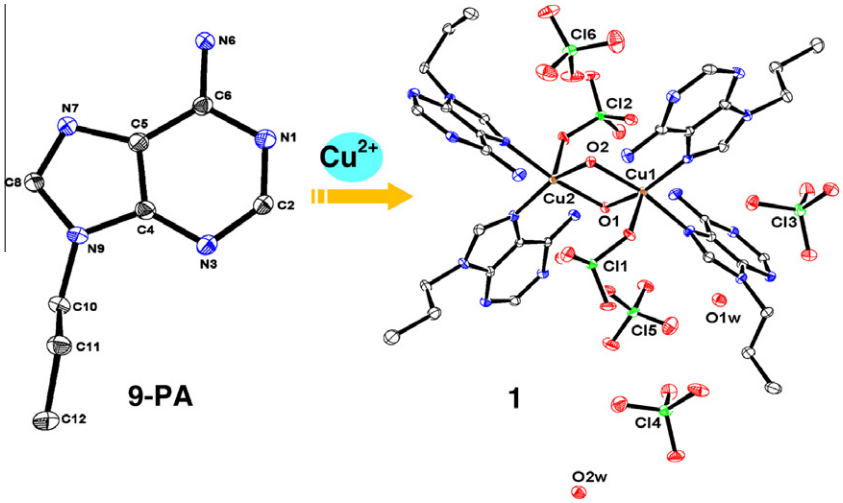

Fig. 1. ORTEP diagram of the asymmetric unit of **1** $[Cu_2(\mathbf{LH^+})_4(OH)^-_2(ClO_4)^-_6(H_2O)_2]$ with 35% ellipsoid probability.

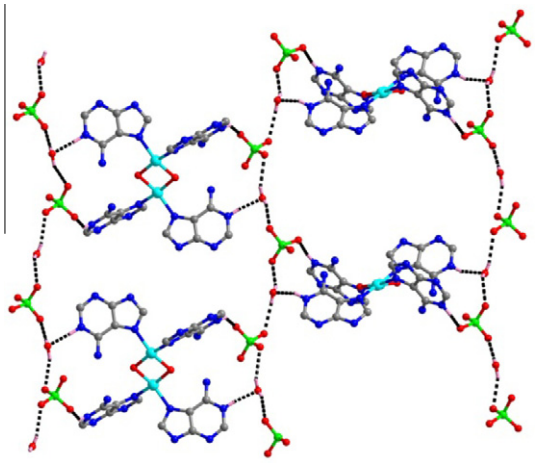

Fig. 2. Hydrogen bonding interaction between N6H and N1H with solvent molecules and anions connecting two discrete units.

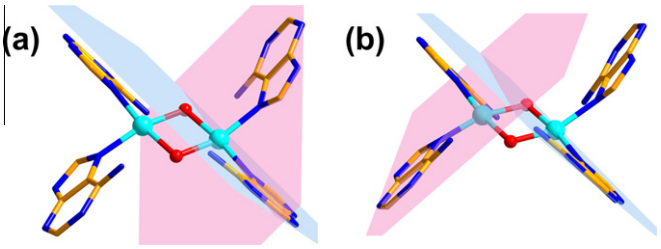

Fig. 4. Representation of dihedral angle in **1** for adenine moieties positioned in *cis* fashion in the dinuclear tetrameric motif. (a) When present on same copper ion. (b) When present at different copper.

MBTH adduct was monitored at 492 nm ($\varepsilon = 3.13 \times 10^4\ M^{-1}\ cm^{-1}$) [8].

2.3.3. 4-*t*-Butylcatechol oxidation

Solutions of 4-*t*-butylcatechol (5–20 mM) were prepared in 50% aq. methanol, containing 10% DMF. Similar assay conditions were followed as described above. The quinone–MBTH adduct was monitored at 494 nm ($\varepsilon = 3.25 \times 10^4\ M^{-1}\ cm^{-1}$) [7].

2.3.4. L-DOPA oxidation

Solution of L-DOPA (0.2–0.8 mM) were prepared in 0.01 M *N*-ethylmorpholine buffer (pH 7.5, prepared in 80% aq. methanol). 10 μL of hydrogen peroxide (30% w/v) was added just before the addition of catalyst. The formation of MBTH–quinone adduct was monitored at 500 nm ($\varepsilon = 1.34 \times 10^4\ M^{-1}\ cm^{-1}$) [9].

2.3.5. Tyrosine oxidation

Solution of tyrosine (0.4–1.0 mM) were prepared in 0.01 M *N*-ethylmorpholine buffer (pH 7.5, prepared in 80% aq. methanol).

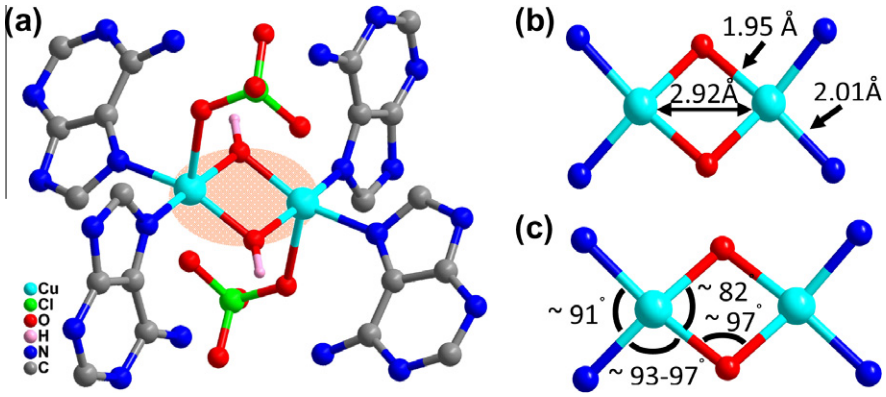

Fig. 3. (a) Representation of discrete unit in **1** where the highlighted portion reveals the presence of Cu_2O_2 entity. (b) and (c) Pictorial representation of important bond distances and angles, respectively, in Cu_2O_2 entity as observed in crystal lattice of **1**.

Table 3
Comparison of bond distances (Å) and angles (°) of Cu_2O_2 core unit in **1** and met-II form of copper-bound tyrosinase enzyme [7e].

Bond distance (Å)			Bond angle (°)		
Atoms	**1**	Enzyme	Atoms	**1**	Enzyme
Cu–Cu	2.92	3.13	Cu–μO–Cu	~97.3	~99.74
Cu–μO	~1.94	~2.05	N–Cu–μO	~94.7	~93.68
Cu–N	~2.00	~2.27	μO–Cu–μO	~82.6	~76.28
			N–Cu–N	~90.8	~90.62

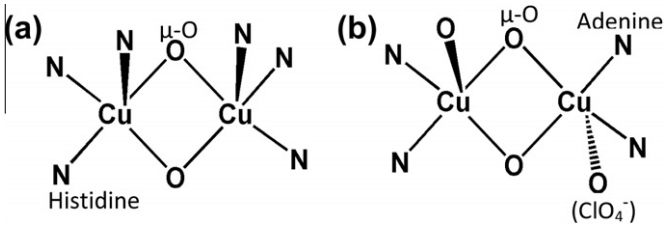

Scheme 3. Schematic representation of Cu_2O_2 core unit in: (a) met-II form of copper-bound tyrosinase enzyme [7e]. (b) in **1**.

10 μL of hydrogen peroxide (30% w/v) was added just before the addition of catalyst. The formation of MBTH–quinone adduct was monitored at 500 nm ($\varepsilon = 1.34 \times 10^4\ M^{-1}\ cm^{-1}$) [9].

2.3.6. X-ray crystallography

Single Crystal of 9-PA and **1** were coated with light hydrocarbon oil and mounted in the 100 K dinitrogen stream of a Bruker SMART APEX CCD diffractometer equipped with CRYO Industries low-temperature apparatus and intensity data were collected using graphite-monochromated Mo Kα radiation. The data integration and reduction were processed with the SAINT software [10]. An absorption correction was applied [11]. Structures were solved by the direct method using SHELXS-97 and refined on *F*2 by a full-matrix least-squares technique using the SHELXL-97 program package [12]. Non-hydrogen atoms were refined anisotropically. In the refinement, hydrogens were treated as riding atoms using the SHELXL default parameters. Crystal structure refinement parameters are given in Table 1 whereas H-bonding parameters are provided in Table 2.

3. Results and discussion

Crystals suitable for X-ray diffraction study for **1** were grown in a month by mixing methanolic solution of ligand with the methanolic solution of copper chloride, in the presence of a few drops of perchloric acid. Crystal analysis of **1** revealed a monoclinic system with *P*21/*n* (No. 1401) as the space group. The asymmetric unit consisted of two copper ions, bridged together through two μ-hydroxyl groups, four N1 protonated adenine moieties coordinated to metal center through N7 nitrogen, six perchlorate counter anions and two water molecules, thereby resulting in a discrete dinuclear motif (Fig. 1).

Table 4
Kinetic data for the catalytic activity of **1** towards phenol oxidation.

Tyrosine	1.71	2.37×10^{-4}	2.62×10^{-4}
4-Hydroxyanisole	38.46	2.28×10^{-4}	2.53×10^{-4}
L-Dopa	0.90	3.94×10^{-4}	4.37×10^{-4}
Catechol	0.08	1.34×10^{-4}	1.49×10^{-4}
4-*t*-Butylcatechol	30.30	1.72×10^{-3}	1.91×10^{-3}

A closer inspection of the crystal lattice revealed hydrogen bonding interactions between N6H and protonated N1H of the adenine moiety with perchlorate anions and water molecules, leading to the formation of an extended lattice structure. The protonated N1 nitrogen of one adenine moiety interacts with percholorate oxygen; the N1H of the other adenine interacts with a water molecule, which is further hydrogen bonded to a percholorate anion. In-space hydrogen bonding interactions between N6H and N1H with perchlorate and water entities permits extended connection of discrete units (Fig. 2).

The hallmark of this structure is the presence of a Cu_2O_2 core unit, where each copper ion exhibits a distorted square pyramidal geometry, as indicated by corresponding τ value being 0.23. The equatorial coordination sites are occupied by two N7 nitrogen atoms from the adenine moieties and two μ-hydroxy oxygen atoms, while the apical position is occupied by the oxygen atom from perchlorate anion (Fig. 3).

It is notable that while N7 nitrogen of adenine residues, copper ions and μ-hydroxy groups lie in one plane, the two perchlorate oxygen atoms are directed towards the opposite ends of the plane. The steric demand of accommodating two adenine moieties at each copper ion does not permit favorable stacking interactions

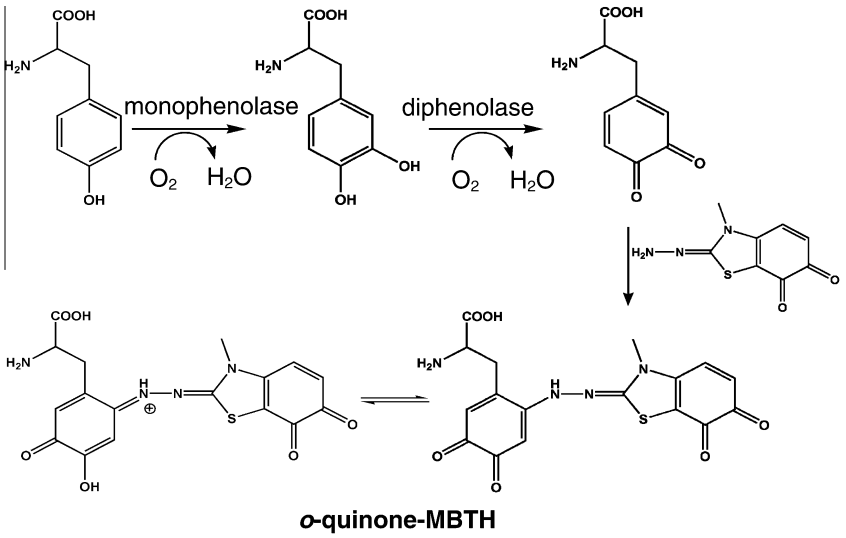

Scheme 2. Schematic representation of the formation of *o*-quinone–MBTH adduct.

between adjacent adenine moieties, as evident from higher dihedral angle between the planes passing through N1, N3, N7 and N9 nitrogen atoms of adjacent nucleobases present in *cis* fashion (~83–89°) (Fig. 4).

We were aware of the fact that dinuclear copper motifs, bridged by oxygen atoms, are integral part of tyrosinase enzyme active site, as well as other type-3 copper enzymes. These enzymes bind oxygen in a 'side-on' fashion, thereby activating it for the enzymatic reaction [13]. Each copper ion present in the active site is also coordinated to three histidine residues, thereby affording a trigonal bipyrimidal geometry around the copper center. It is important to mention that type-3 copper enzymes are EPR inactive [13]. Interestingly, complex **1** was also found to be EPR-silent at 120 K, which suggests for a strong coupling between the two copper atoms and is consistent with doubly bridged structures previously reported [14]. This led us to further compare salient structural details of the copper center in present in redox copper enzymes and **1**.

The dinuclear copper unit present in **1** was compared with the dicopper present in the active site of met-II form of tyrosinase. It is interesting to note that three histidiyl imidazole rings coordinate to the copper center, to afford a penta-coordinated environment (Scheme 3a), whereas perhaps owing to the bulk of adenine rings only two ligands were accommodated around the copper center, while perchlorate anion coordinates to the copper ions (Scheme 3b). Table 3 displays selected bond distances and bond angles in **1** and the met-II form of copper-bound tyrosinase enzyme [13e], indicating remarkable similarities between the two copper centers.

Considerable studies focusing on synthetic models of dinuclear copper core have been designed and tested for the mimicry of catalytic activity present protein enzymes, with much success [15]. Thus, the structural similarity described above provided us an impetus to analyse the catalytic potential of **1** for the oxidation of monophenolic and diphenolic substrates. Three different monophenolic and diphenolic substrates, such as catechol, 4-*t*-butylcatechol and 4-hydroxyanisole were employed, along with their natural analogues, tyrosine and L-DOPA.

However, efforts were not made to fully optimize reaction conditions or for the scale up of products.

A time-dependent formation of corresponding chromogenic MBTH-adduct (formed as a result of reaction between MBTH and the oxidation product, *o*-quinone) was monitored at their respective λ_{max} values (Scheme 2). The adduct formation with the substrates suggested the possibility of both monophenolase and diphenolase catalytic activities for **1**. Table 4 shows the K_m, V_{max} and K_{cat} values for the monophenolic and diphenolic substrates used, as determined from corresponding Lineweaver–Burk plots (Fig. 5). It must be emphasized that exogenous oxidant was not used for synthetic substrates in these reactions. In comparison, the Michaelis–Menten parameters, K_m, and V_{max} for commercial tyrosinase enzyme, using catechol as substrate, were reported as 3.88 mM and 5.29×10^{-4} mM min^{-1}, respectively [8].

Low K_m values were observed for simple diphenols namely catechol and L-DOPA suggesting preferential binding of diphenols to **1**. Introduction of a bulky *t*-butyl group probably hinders the binding interaction with **1**, thus 4-*t*-butylcatechol exhibits higher K_m value. On the other hand 4-hydroxyanisole, a monophenol shows least binding preferences when compared to other diphenols. However, these binding preferences cannot be correlated with observed velocities, thereby making it difficult to establish an unequivocal relationship between binding preferences and the rate of reactions.

We decided to further confirm the oxidation of 4-hydroxyanisole by **1** via an alternate method. In this reaction, the oxidized *o*-diquinone product was reacted with 1,2-phylenediamine in situ and the appearance of resulting adduct was confirmed by mass spectral analysis, thus once again indirectly proving oxidation of a monophenol (ESI).

4. Conclusions

In conclusion, we have presented crystallographic features of copper complex of 9-propyladenine exhibiting a discrete dicopper center around Cu_2O_2 core, an arrangement remarkably similar to

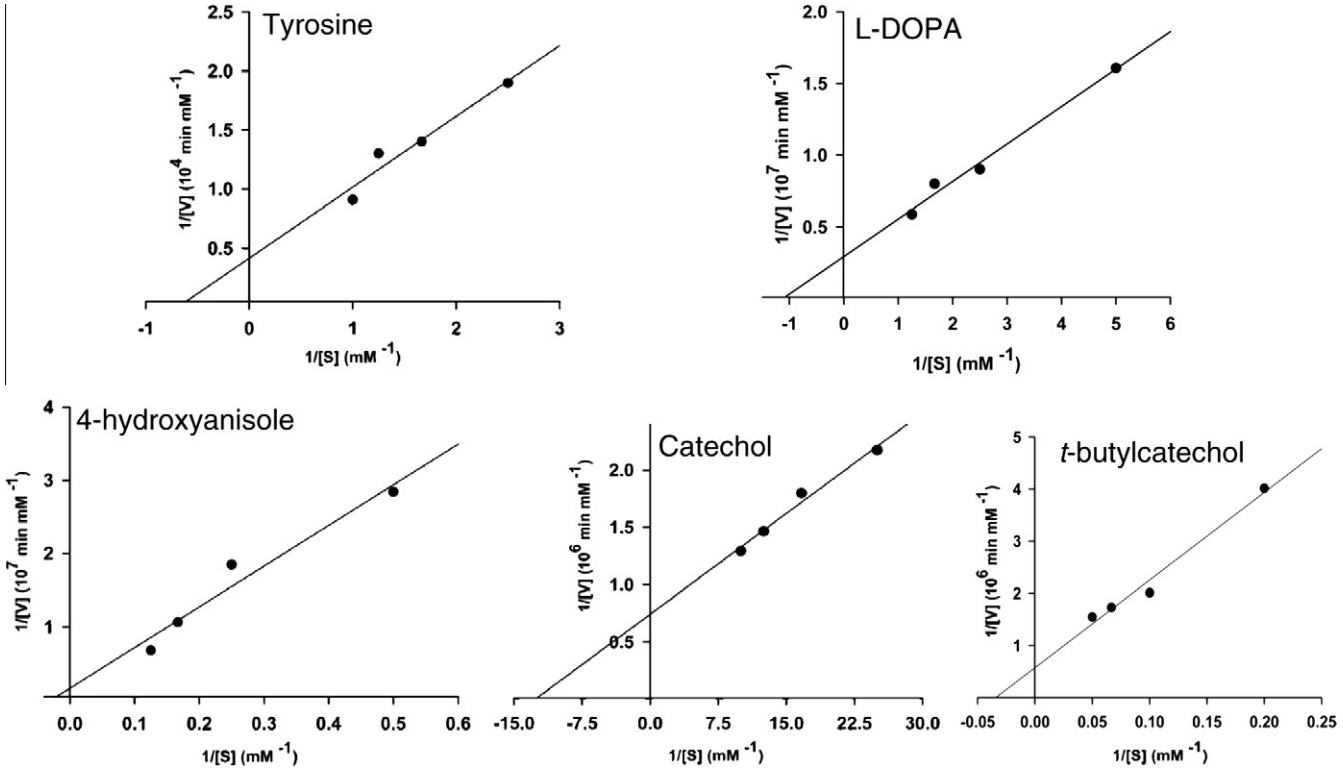

Fig. 5. Lineweaver–Burk plot for Tyrosine, L-DOPA, Catechol, *t*-butylcatechol and 4-hydroxyanisole.

tryosinase actives. This complex also supports the catalysis of phenol oxidation thus raising a possibility of catalytically competent metal-nucleobase systems which perhaps preceded protein enzymes [16].

Acknowledgment

We thank Single Crystal CCD X-ray facility at IIT-Kanpur. This work is financially supported by an Indo-Spain project supported by DST, India.

Appendix A. Supplementary data

CCDC 659665 and 789919 contain the supplementary crystallographic data for this paper. These data can be obtained free of charge via http://www.ccdc.cam.ac.uk/conts/retrieving.html, or from the Cambridge Crystallographic Data Centre, 12 Union Road, Cambridge CB2 1EZ, UK; fax: (+44) 1223-336-033; or e-mail: deposit@ccdc.cam.ac.uk. Supplementary data associated with this article can be found, in the online version, at http://dx.doi.org/10.1016/j.poly.2012.05.013.

References

[1] (a) H. Sigel, Chem. Soc. Rev. 22 (1993) 255;
(b) S. Sivakovaa, S.J. Rowan, Chem. Soc. Rev. 34 (2005) 9;
(c) J.A.R. Navarro, B. Lippert, Coord. Chem. Rev. 185–186 (1999) 653;
(d) R.K.O. Sigel, H. Sigel, Acc. Chem. Res. 43 (2010) 974;
(e) Z. Szabó, Coord. Chem. Rev. 252 (2008) 2362.
[2] R. Breslow, J. Mol. Catal. 91 (1994) 161.
[3] (a) J.-L. Décout, J. Vergne, M.C. Maurel, Macromol. Chem. Phys. 196 (1995) 2615;
(b) F. Bruston, J. Vergne, L. Grajcar, B. Drahi, R. Calvayrac, M.H. Baron, M.C. Maurel, Biochem. Biophys. Res. Commun. 263 (1999) 672.
[4] (a) J. Vergne, L. Dumas, J.-L. Décout, M.C. Maurel, Planet Space Sci. 48 (2000) 1139;
(b) S.G. Srivatsan, M. Parvez, S. Verma, Chem. Eur. J. 8 (2002) 5184;
(c) S.G. Srivatsan, S. Verma, Chem. Commun. (2000) 515;
(d) S.G. Srivatsan, S. Verma, Chem. Eur. J. 7 (2001) 828;
(e) C. Madhavaiah, S.G. Srivatsan, S. Verma, Catal. Commun. 2 (2001) 95;
(f) J.L. García-Giménez, G. Alzuet, M. González-Álvarez, A. Castiñeiras, M. Liu-González, J. Borrás, Inorg. Chem. 46 (2007) 7178.
[5] (a) C.S. Purohit, S. Verma, J. Am. Chem. Soc. 128 (2006) 400;
(b) C.S. Purohit, A.K. Mishra, S. Verma, Inorg. Chem. 46 (2007) 8493;
(c) C.S. Purohit, S. Verma, J. Am. Chem. Soc. 129 (2007) 3488;
(d) C.S. Purohit, A.K. Mishra, S. Verma, CrystEngComm 10 (2008) 1296;
(e) J. Kumar, S. Verma, Inorg. Chem. 4 (2009) 6350;
(f) A.K. Mishra, C.S. Purohit, J. Kumar, S. Verma, Inorg. Chim. Acta 362 (2009) 855;
(g) M.D. Pandey, A.K. Mishra, V. Chandrasekhar, S. Verma, Inorg. Chem. 49 (2010) 2020;
(h) A.K. Mishra, S. Verma, Inorg. Chem. 49 (2010) 3691;
(i) A.K. Mishra, S. Verma, Inorg. Chem. 49 (2010) 8012;
(j) A.K. Mishra, R.K. Prajapati, S. Verma, Dalton Trans. 39 (2010) 10034;
(k) A.K. Mishra, J. Kumar, S. Khanna, S. Verma, Cryst. Growth Des. 11 (2011) 1623;
(l) R.K. Prajapati, S. Verma, Inorg. Chem. 50 (2011) 3180.
[6] S. Verma, A.K. Mishra, J. Kumar, Acc. Chem. Res. 43 (2010) 79.
[7] P. Chaudhuri, M. Hess, T. Weyhermuller, K. Wieghardt, Angew. Chem., Int. Ed. 38 (1999) 1095.
[8] J.C. Espin, J. Tudela, F. Garcia-Canovas, Anal. Biochem. 259 (1998) 118.
[9] (a) C.A. Claussen, E.C. Long, Chem. Rev. 99 (1999) 2797;
(b) C.J. Burrows, J.G. Muller, Chem. Rev. 98 (1998) 1109.
[10] SAINT+, 6.02 ed., Bruker AXS, Madison, WI, 1999.
[11] G. M. Sheldrick, SADABS 2.0, University of Göttingen, Göttingen, Germany, 2000.
[12] G.M. Sheldrick, SHELXL-97, Program for Crystal Structure Refinement, University of Göttingen, Göttingen, Germany, 1997.
[13] (a) A.G. Martin, F. Depoix, M. Stohr, U. Meissner, S. Hagner-Holler, K. Hammouti, T. Burmester, J. Heyd, W. Wriggers, J. Markl, J. Mol. Biol. 366 (2007) 1332;
(b) T. Klabunde, C. Eicken, J.C. Sacchettini, B. Krebs, Nat. Struct. Biol. 5 (1998) 1084;
(c) C. Eicken, F. Zippel, K. Buldt-Karentzopoulos, B. Kreb, FEBS Lett. 436 (1998) 293;
(d) Y. Matoba, T. Kumagai, A. Yamamoto, H. Yoshitsu, M. Sugiyama, J. Biol. Chem. 281 (2006) 8981;
(e) H. Decker, T. Schweikardt, F. Tuczek, Angew. Chem., Int. Ed. 45 (2006) 4546;
(f) M. Sendovski, M. Kanteev, V. S. Ben-Yosef, N. adir, A. Fishman, Acta Crystallogr., Sect. F66 (2010) 1101–1103.;
(g) C. Gerdemann, C. Eicken, B. Krebs, Acc. Chem. Res. 35 (2002) 183;
(h) R.J. Deeth, C. Diedrich, J. Biol. Inorg. Chem. 15 (2010) 117;
(i) C. Olivares, F. Solano, Pigment Cell Melanoma Res. 22 (2009) 750;
(j) E.I. Solomon, R.G. Hadt, Coord. Chem. Rev. 255 (2011) 774.
[14] (a) S. Torelli, C. Belle, I. Gautier-Luneau, J.L. Pierre, E. Saint-Aman, J.M. Latour, L. Le-Pape, D. Luneau, Inorg. Chem. 39 (2000) 3526;
(b) A. Banerjee, R. Singh, E. Colaacio, K.K. Rajak, Eur. J. Inorg. Chem. 2009 (2009) 277;
(c) A. Banerjee, S. Sarkar, D. Chopra, E. Colaacio, K.K. Rajak, Inorg. Chem. 47 (2008) 4023;
(d) A. Mukherjee, F. Lloret, R. Mukherjee, Inorg. Chem. 47 (2008) 4471;
(e) E. Peyroux, W. Ghattas, R. Hardé, M. Giorgi, B. Faure, A.J. Simaan, C. Belle, M. Réglier, Inorg. Chem. 48 (2009) 10874;
(f) M. González-Álvarez, G. Alzuet, J. Borrás, S. Gracía-Granda, J.M. Montejo-Bernardo, J. Inorg. Biochem. 96 (2003) 443.
[15] (a) I.A. Koval, P. Gamez, C. Belle, K. Selmeczi, J. Reedijk, Chem. Soc. Rev. 35 (2006) 814;
(b) S. Itoh, H. Kumei, M. Taki, S. Nagatomo, T. Kitagawa, S. Fukuzumi, J. Am. Chem. Soc. 123 (2001) 6708;
(c) L.M. Mirica, M. Vance, D.J. Rudd, B. Hedman, K.O. Hodgson, E.I. Solomon, T.D.P. Stack, J. Am. Chem. Soc. 124 (2002) 9332;
(d) L.Q. Hatcher, K.D. Karlin, Adv. Inorg. Chem. 58 (2006) 131;
(e) G. Battaini, A. Granata, E. Monzani, M. Gullotti, L. Casella, Adv. Inorg. Chem. 58 (2006) 185;
(f) A. De, S. Mandal, R. Mukherjee, J. Inorg. Biochem. 102 (2008) 1170;
(g) C.J. Cramer, W.B. Tolman, Acc. Chem. Res. 40 (2007) 601;
(h) R. Malte, S. Julia, T. Felix, J. Coordin. Chem. 63 (2010) 2382;
(i) I. Solomon, U.M. Sundaram, T.E. Machonkin, Chem. Rev. 96 (1996) 2563;
(j) E.A. Lewis, W.B. Tolman, Chem. Rev. 104 (2004) 1047;
(k) L.M. Mirica, X. Ottenwaelder, T.D.P. Stack, Chem. Rev. 104 (2004) 1013;
(l) K. Selmeczi, M. Réglier, M. Giorgi, G. Speier, Coordin. Chem. Rev. 245 (2003) 191;
(m) S. Herres-Pawlis, P. Verma, R. Haase, P. Kang, C.T. Lyons, E.C. Wasinger, U. Flörke, G. Henkel, T.D.P. Stack, J. Am. Chem. Soc. 131 (2009) 1154;
(n) D. Venegas-Yazigi, D. Aravena, E. Spodine, E. Ruiz, S. Alvarez, Coordin. Chem. Rev. 254 (2010) 2086;
(o) M. Rolff, J. Schottenheim, H. Decker, F. Tuczek, Chem. Soc. Rev. 40 (2011) 4077;
(p) I.G. Bosch, A. Company, J.R. Frisch, M.T. Sucarrat, M. Cardellach, I. Gamba, M. Güell, L. Casella, L. Que Jr., X. Ribas, J.M. Luis, M. Costas, Angew. Chem. Int. Ed. 49 (2010) 2406.
[16] (a) M.P. Callahan, K.E. Smith, H.J. Cleaves II, J. Ruzicka, J.C. Stern, D.P. Glavin, C.H. House, J.P. Dworkin, Proc. Natl. Acad. Sci. 108 (2011) 13995;
(b) M.-C. Maurel, J.-L. Decout, Tetrahedron 55 (1999) 3141;
(c) T.J. Wilson, D.M.J. Lilley, Science 323 (2009) 1436;
(d) L.E. Orgel, Crit. Rev. Biochem. Mol. 39 (2004) 99.